Netherlands Journal of Geosciences

Original Article

Cite this article: Roel Dijksma and Brian Ramirez-Cortes. Erosion mitigation testing for a small brook system under human influences in South Limburg, the Netherlands: a field and HEC-RAS modelling approach. *Netherlands Journal of Geosciences*, Volume 105, e14028. https://doi.org/10.70712/NJG.v105.14028

Received: 3 February 2026
Revised: 9 July 2026
Accepted: 28 July 2026
Published: 2 September 2026

Keywords:
deeply incised brooks; sediment transport; morpho-dynamics; HEC-RAS; gabion dams; armouring layers; erosion mitigation

Corresponding author:
Roel Dijksma,
roel.dijksma@wur.nl

Erosion mitigation testing for a small brook system under human influences in South Limburg, the Netherlands: a field and HEC-RAS modelling approach

Roel Dijksma[1] and Brian Ramirez-Cortes[2]

[1]Hydrology and Environmental Hydraulics Group, Wageningen University, Wageningen, the Netherlands; [2]Soil Geography and Landscape Group, Wageningen University, Wageningen, the Netherlands

Abstract

Riverine ecosystems with a surface water gradient of >0.01 m/m have the tendency to be of erosional character, with the potential to greatly alter surface and subsurface hydrological fluxes. Primarily, the degree of erosion is strongly related to the bed material and the frequency and magnitude of peak flow discharges. However, given the increasing environmental risks associated with climate change and land use changes, erosional processes are expected to intensify. Thus, investigating these processes in hydrologically and ecologically complex areas remains critical, as their susceptibility can be particularly high.

This paper studies the Noor brook and the adjacent upward-seepage-dependent Natura 2000 ecosystem in the south of the Netherlands, to explore channel erosional processes and mitigation practices in hydrogeologically highly complex environments. This small brook is one of many in the area facing peak flow discharges associated with heavy rainfall and sewage water overflow. When the brook would completely cut through the poorly permeable clayey valley filling, it is expected that more seepage water will flow directly into the Noor brook. In turn, this will reduce the calcium carbonate-rich seepage water for the Noorbeemden causing a detrimental impact on the ecological value of the area.

Extensive field studies have been conducted regarding the local geomorphology of the brook and the local hydrogeology, including hydrological experiments on seepage, sewage and rain water. Here, we conduct a sediment transport and modelling study to deepen the understanding of the impact of erosion mitigation practices on the hydraulics and morphodynamics of the Noor brook. This way, the response of the Noor to further bedload erosion was assessed through shear stress analysis. Gravel armouring and gabion dams were incorporated into 1D steady and quasi-unsteady simulations through the Hydrologic Engineering Center's River Analysis System (HEC-RAS) modelling software. Lastly, modeling results regarding sediment transport dynamics were used to estimate the response of deep and shallow groundwater levels on mitigation measures.

For erosion mitigation purposes, the identification of areas susceptible to deep incision was found to be closely linked to the magnitude of the peak discharge and the morphology of the brook. The river gradient was found to have major contributions to accelerating deep incisions in the Noor brook. Gabion dams and gravel armouring showed contrasting results in erosion dynamics based on the magnitude of their application. Yet, such practices could potentially benefit groundwater levels at the riverine scale when properly implemented. All in all, the combination of field and HEC-RAS modelling exercises showed that, within reasonable limits, the erosional behaviour of small riverine ecosystems can be understood, as well as the impact of mitigation practices.

Introduction

Hydrological erosion – often caused by human influence – plays a crucial role in the morphological development of rivers of all sorts of sizes and shapes (Knighton, 2014; Moreno Gómez et al., 2025). Such erosion can lead to drastic changes in the riverbed, both vertically and horizontally, strongly influencing feedbacks between hydrodynamics, sediment transport and channel morphology in river systems (Zhou, 2017). These changes can be gradual (landscape evolutions) or abrupt (landscape revolutions).

In the Netherlands, especially in the more elevated southeastern part of the country, multiple stream valleys suffer from the erosive power of the stream flow (Website: Natura2000.nl, 2025). The combination of a brook bed consisting of fine-grained

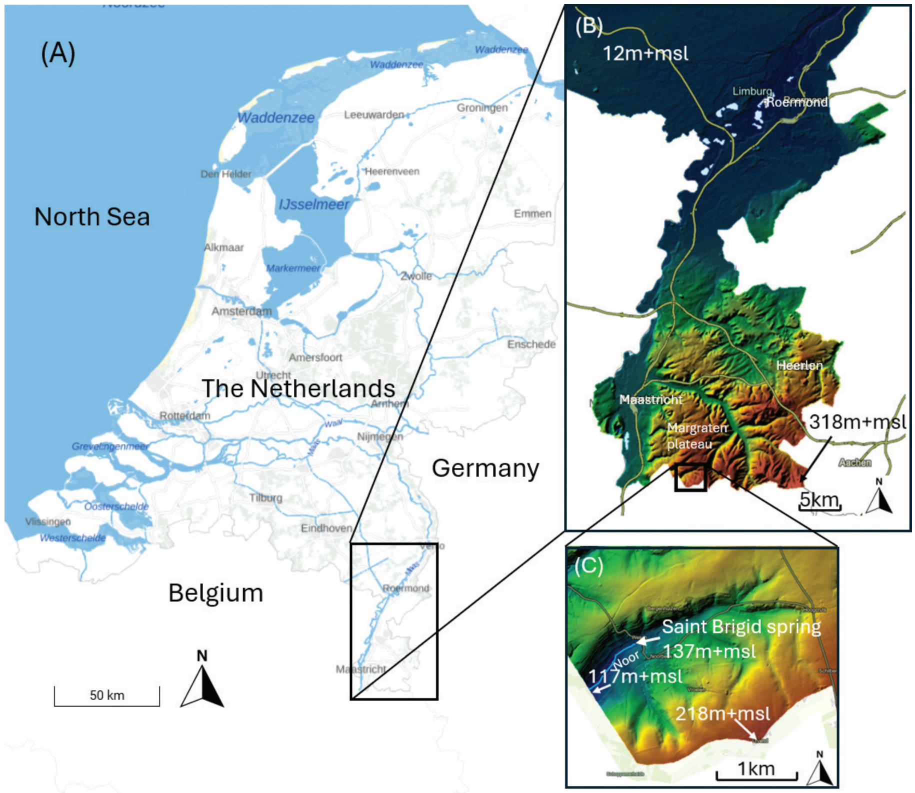

Figure 1. (A) Geographical location of the study area in the southernmost part of the Netherlands; (B) topography of the southern part of the Netherlands; (C) topography of the Noor brook valley and adjacent Noorbeemden nature reserve (modified from website Arcgisonline.nl, 2025).

unconsolidated material and a riverbed slope of >0.01 m/m already creates an erosive behaviour. Due to an increased risk of intense precipitation events (extreme in intensity and/or total volume), the erosion has accelerated over the last decades.

One of the heavily affected streams is the Noor brook, located at the southwest of the Margraten Plateau, close to the Dutch-Belgian border (see Figure 1). Due to its bed bottom slope of 0.017 m/m and the silty/clayey composition of the valley filling, the brook is cutting into its sediments. The erosion during relatively short-lasting but intense peak discharges means that the Noor has been carving even faster into the valley filling (Dijksma & Van Lanen, 2001). Current river incisions measure on average ~ 1.5 m, varying between 1 and 3 m due to the local topography.

While the hydrogeological dynamics of the region are well documented (Van Lanen & Dijksma, 1999), only recent studies have started to address the morphodynamics of the brook and mitigation strategies to prevent further incision (Woolderink & Harkema, 2023). In particular, pilot studies have examined the effect of small and large wood debris jams on channel morphodynamics (Campuzano, 2017; Mesman, 2019). Although wood jams provide stability to channel morphology and promote deposition of fine material in the short term, they might also contribute to patches of scour through flow convergence (Campuzano, 2017; Manners et al., 2007; Mesman, 2019; Wallerstein et al., 1997). Previous studies have also highlighted long-term uncertainties such as decomposition of organic material and as such reduced hydraulic resistance and changing flow dynamics (Grabowski et al., 2019; Roni et al., 2015). This suggests that they represent a temporal solution for channel erosion. Therefore, in light of exploring more permanent river restoration solutions in the Noor and controlling further riverbed incision, a comprehensive understanding of how channel morphodynamics respond to long-term erosion mitigation practices is required. Such understanding must account for the geomorphic relevance of hydrological events based on their magnitude and frequency of occurrence.

Gravel armouring (a protective layer of a mix of gravel and fine material) is a common practice for improving the geomorphic condition of sediment starved brook reaches. This armouring layer also counteracts further bed incision (Chardon et al., 2021). Several studies have reported positive ecological responses, including increased taxonomic richness of macroinvertebrates (Staentzel et al., 2018) and the rehabilitation of spawning habitats for lithophilic fish species (Pasternack et al., 2004). Additionally, other studies (Merz & Ochikubo Chan, 2005) have shown that benthic macroinvertebrates can colonise new gravels quickly. While armouring materials can be locally sourced, it is important to consider a well-graded sediment mixture of sands, silts and gravels in order to provide a structurally stable yet variable riverbed (Pitlick et al., 2008). Gabion dams represent a second solution to reduce erosive processes in the brook bed. Regular impermeable dams have the disadvantage that they cut the brook bed into segments, which has impact on the aquatic ecology. However, due to the porous nature of gabion dams, these structures partially block the water flow, reducing the flow velocity and promoting the deposition of surface runoff sediments (Hariri et al., 2022).

The creation of gabion dams (Vaezi et al., 2021) and armouring layers (Ikhsan et al., 2022; Wang et al., 2020) in a vulnerable ecosystem like the Noor-Noorbeemden necessitates a thorough preparation and a test to determine whether these

https://doi.org/10.70712/NJG.v105.14028

measures have the desired impact and whether they will not be eroded as well. Therefore, this study aimed at conducting a sediment transport and modelling study through HEC-RAS model in order to investigate the erosion and sedimentation processes in the riverbed of the Noor brook. Consequently, this study integrates hydrogeological information to assess the implications of gabion dams and gravel armouring for the integrity of groundwater fluxes in the Noorbeemden. The modelling results will be used for the setup of a pilot project where a segment of approximately 100 m will be used to test the impact of adding an infill in combination with an armouring layer and a gabion dam.

Materials and methods

Area description

The Noor brook is a 3.1 km long watercourse lying at the base of a fragmented plateau landscape called Margraten Plateau, into which multiple dry valleys converge and discharge. The brook originates in the village of Noorbeek at the St. Brigid spring at an altitude of 137 m+msl and meanders southwest towards Belgium. Figure 1 shows the location of the Noor brook and the adjacent Noorbeemden nature reserve in the southernmost part of the Netherlands and its topography. Additionally, Figure 2 shows an in-channel view of the Noor brook, as the most deeply incised fluvial section in the Dutch part of the brook (picture taken in February 2022).

Deep incision of the brook bed has the potential to negatively affect the ecology of the riparian area known as 'De Noorbeemden'. This Natura 2000 reserve area encompasses a diverse yet fragile ecosystem which is highly dependent on the calcium carbonate ($CaCO_3$)-rich upward seepage. When the incision cuts through the remaining water-resistant clay layer, it is expected that a large portion of the seepage will directly flow into the brook (see also Figure 5). As a result, the water type in the root zone of the Noorbeemden might shift from $CaCO_3$-rich seepage water to rainwater type.

Regional hydrogeology

The regional hydrogeology is best explained by, at first, a glance at the regional geology and the hydrological base, followed by

Figure 2. Heavily eroded brook bed in the Dutch region of the Noor brook. Fluvial erosion has deepened and widened the brook considerably over the last decades due to (1) landscape evolution during average discharge and (2) landscape revolution during short intensive peak discharges. It is estimated that approximately 2 m of the depth is due to erosion and 0.5 m is related to microtopography (floodplain aggradation). In the front, some degraded remains of a woody debris jam are visible. The gravel underneath the wood debris was artificially added as armouring layer to avoid deep scours.

a closer look at the Noor brook and Noorbeemden. Figure 3 shows a simplified geological cross section B-B′ in a northwest-southeast direction from Maastricht to the Dutch-Belgian border near De Planck. The oldest formations in the region are Upper-Carboniferous highly consolidated shales and sandstones (Van Lanen & Dijksma, 1999). This formation is impermeable and thus forms the hydrogeological base of the region.

The Carboniferous rocks are overlain by a series of poorly consolidated Upper-Cretaceous formations. The **Aachen Formation** consists of poorly consolidated sandstone and acts as an aquifer. However, this formation is limited in thickness

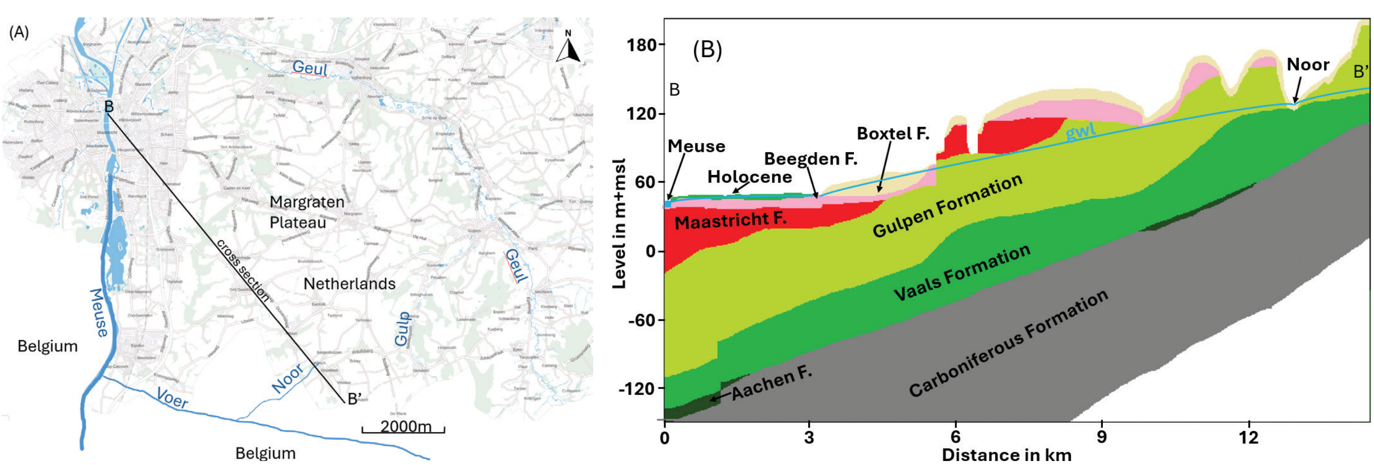

Figure 3. (A) Location of geological cross section B-B′ in South Limburg.; (B) Geological setting of the study area (adapted from Website: Dinoloket.nl, 2025) including a reference line for the groundwater level (gwl). The colours indicate the various geological formations.

and spatial distribution and thus plays no role in the Noor region. The **Vaals Formation** has developed as a near-coast mudflat with siltstone and interbedded sandstone. Fractured interbedded sandstones have a limited share in the total volume of the mudflat deposits in general but can be the most important contributor to the groundwater flow in this layer (Dijksma & Van Lanen, 2001). The horizontal secondary hydraulic conductivity (k_h) of these fractured sandstones is estimated as 20 m/d, where the siltstones have an estimated k_h of ≤0.8 m/d (Dijksma & Van Lanen, 2001; Van Lanen et al., 1995). With a weighted average k_h of 1.5 m/d and an average thickness of 50 m in the Noor catchment, the transmissivity (*kD*) of the Vaals Formation is estimated as 75 m^2/d, which makes it the most important aquifer (Van Lanen et al., 1995). The **Gulpen Formation** was formed in a deeper sea and consists of soft medium-grained chalk (calcarenite) with an average k_h of 2.5 m/d. The **Maastricht Formation**, i.e. the youngest Upper-Cretaceous formation in the region has been completely eroded in the Noor catchment and only plays a role in groundwater flow further northwest. The **Beegden** and **Boxtel Formations** are predominantly high in the landscape and do not play a role in horizontal water flow.

Groundwater levels (gwl, Figure 3) under the plateau can be several tens of m below surface level. The thick unsaturated zone is causing a delayed and attenuated response of the groundwater level under the plateau on the rain surplus. The groundwater from the Margraten Plateau will predominantly be discharged to the main rivers Meuse, Geul and Gulp, which are surrounding the Margraten Plateau (see Figure 3). A relatively small portion is finding its way to the Noor brook. Both Gulpen and Vaals F. can act as aquifer for that, but since the saturated thickness of Gulpen F. is limited, Vaals F. is considered the most important aquifer.

Local hydrogeology

Figure 4 zooms in to the Noor area and shows a 1000 m N-S cross section. The regolith layer in Figure 4 is the weathering residue from the underlying geological formation, being either Gulpen F., Vaals F., or locally mixed with remnants of overlying formations which have been eroded over time. From all the sediments

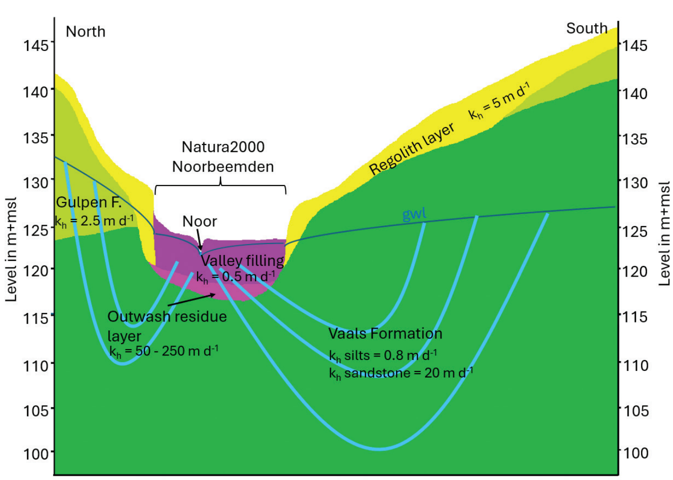

Figure 4. Indicative hydrogeological cross section over the Noor brook and adjacent valley flanks (modified from Van Lanen et al., 1995). Blue lines indicate the flow routes in the saturated zone.

previously accumulated in the deep valley, the finer material was washed out by the Noor at the final stages of the last ice age (Weichselian). As a result, coarser particles such as the gravels from Beegden F. and flintstones from Gulpen F. formed an outwash residue. During Holocene, predominantly from the Roman era onwards, finer grained sediments were deposited in the deepest part of the brook valley due to deforestation and agricultural activity. The lower parts of this valley filling consist predominantly of clayey material. The upper parts of the valley filling are in the silty loam range with some more sandy beds (former brook beds) and some gravel (Van Lanen et al.., 1995).

Impact of deep incision

Figure 5 zooms further into a N-S 300 m transect, to give a closer look at what the impact would be when the brook would cut through the clayey lower part of the valley filling. The blue arrows which represent seepage flow routes are indicative and show that a relatively large portion would seep directly into the brook, leaving less water to create $CaCO_3$-rich seepage in the root zone in the Noorbeemden. The red arrows represent rainfall infiltrating into the root zone. Figure 5A represents the current (2025) situation where the incision did cut completely through the silty upper part of the valley filling and has started to erode the poorly permeable dense clay layer. The vertical hydraulic resistance (c) of this clay layer depends on the thickness and the vertical hydraulic conductivity (k_v). Since the thickness and k_v are expected to be rather variable because of the variable conditions during deposition in space and time, *c* is also expected to vary significantly in a range of ~500 – ~2000 days (Van Lanen et al., 1995). As a result, the piezometric head in Vaals F. reaches levels well above surface level (artesian conditions, Figure 5A). That artesian water level varies because of variable meteoric conditions, but has been declining from on average 1.5 m above surface level in the 1990s to 0.5 m above surface level in 2025 (see Figure 12). This reduced head in the deeper aquifer is already causing a reduced $CaCO_3$-rich seepage flux towards the root zone in the Noorbeemden. However, electrical conductivity measurements in shallow piezometers at variable distances from the deeply incised brook reveal that seepage water is still dominant in the root zone (EC values ranging from 600 to 800 μS/cm), except for a ~5 m wide strip close to the brook (Kessels, 2012; Tiernego, 2010). Close to the deep incision, rainwater starts to become dominant in the root zone.

Figure 5B represents a situation where the brook would completely cut through the clay layer and into the gravel layer underneath (the outwash residue). Under these conditions, the flow from Vaals F. upward can horizontally redistribute in the gravel layer and cause increased flow to the brook directly. The seepage fluxes up to the root zone in the Noorbeemden will then decrease and rainwater has the option to infiltrate because of reduced pressure from below (red arrows in Figure 5B). This change in water type from seepage water to rain water in the root zone might impact the vegetation composition.

Climate and Noor brook peak discharge

The study area is characterised by a temperate marine climate (Cfb to the Köppen Geiger classification). Averaged annual precipitation is in the order of 750 mm (Website: KNMI.nl, 2025). Highest daily precipitation was measured on 27 August 1971 with >100 mm, but the single event precipitation measured on 14 and 15 July 2021 with a total of 150 mm did put even more hydrological stress on the

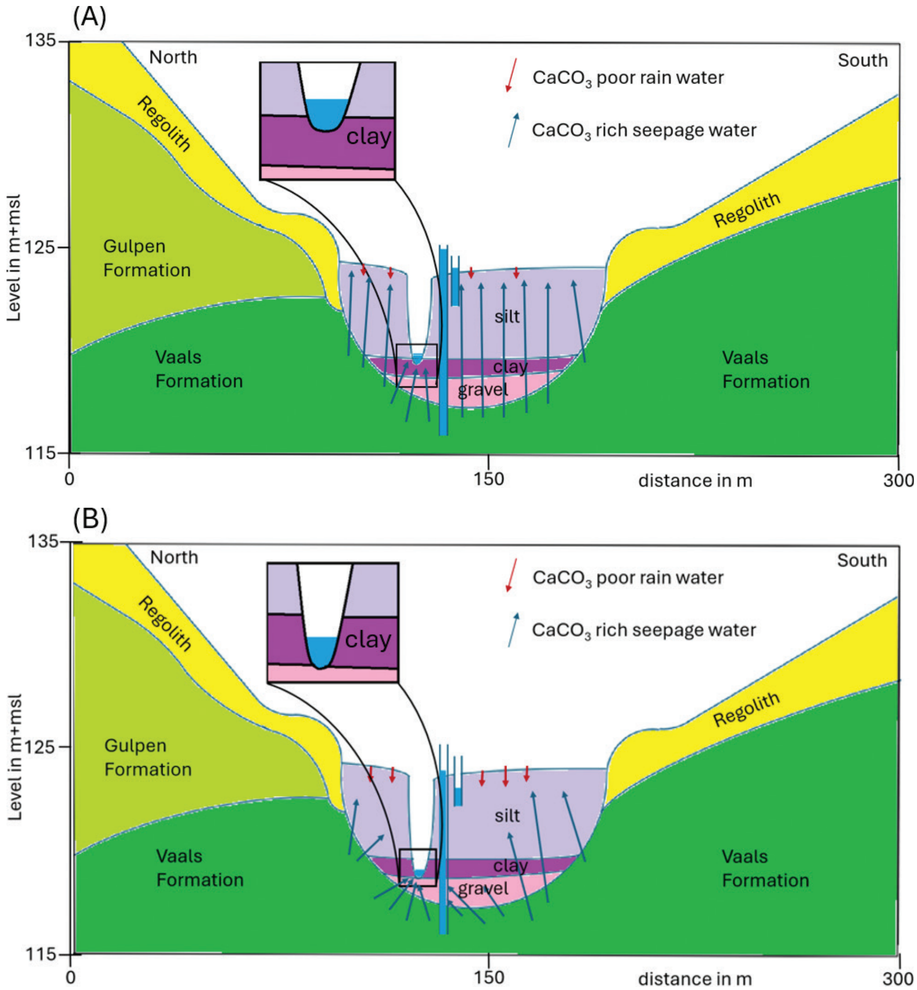

Figure 5. Detailed N-S cross section over the Noor brook with (A) current (2025) situation where the brook starts to incise into the poorly permeable valley fill clay and (B) possible future situation where the brook did cut through the valley fill clay and taps into the highly permeable gravel layer. Blue arrows indicate $CaCO_3$-rich seepage water flow routes and red arrows indicate $CaCO_3$-poor rain water flow routes.

landscape. Over the time period 2019–2023, at least 7–10 large discharge peaks per year related to heavy precipitation were recorded, where the July 2021 rain event triggered by far the largest discharge peak (see Figure 6).

Field data collection and manipulation

In line with the concept of Lane's diagram regarding channel degradation and aggradation (Vanoni, 1975), information on the flow discharge, brook bed slope and sediment size was collected in the field to quantify the current susceptibility of the Noor to vertical erosion during peak flow discharges.

In order to estimate the flow hydrograph, the Manning equation (Equation 1) was applied to the water level record of a monitoring well placed in the brook, utilising detailed information on brook morphology from Woolderink and Harkema (2023), including a set of channel cross-sectional profiles. From this dataset, the brook wetted area associated with specific water levels was calculated. Additionally, a bed bottom slope of 0.017 m m^{-1} was calculated for a 50 m segment encompassing the monitoring well. Based on the current condition of the Noor brook, the Manning coefficient was set to 0.04 s/m$^{1/3}$ (Dust & Wohl, 2012).

$$Q = \frac{1}{n} \cdot S^{1/2} \cdot A \cdot R^{2/3} \qquad \text{Equation 1}$$

Where:
Q = discharge (m^3/s)
n = Manning coefficient (s/m$^{1/3}$)
S = slope of the energy grade line (–)
A = cross-sectional wetted area (m^2)
R = hydraulic radius (m)

The resulting hydrograph was analysed using the Flow Duration Curve (FDC) approach to evaluate the magnitude and duration of flow discharge events and their distribution over the specified time period. Given the nature of the flow conditions, distinction was made between base flow (low flow) and peak flow (high flow) conditions. Low-flow conditions were represented by flow discharge events with a probability of occurrence of 95%, while high-flow conditions were associated with a probability of occurrence of 5%. Two flow discharges were targeted: (1) the highest peak flow discharge pertaining to the exceptional rainfall event in July 2021; and (2) the median peak flow discharge associated with the 5% highest water levels recorded.

https://doi.org/10.70712/NJG.v105.14028

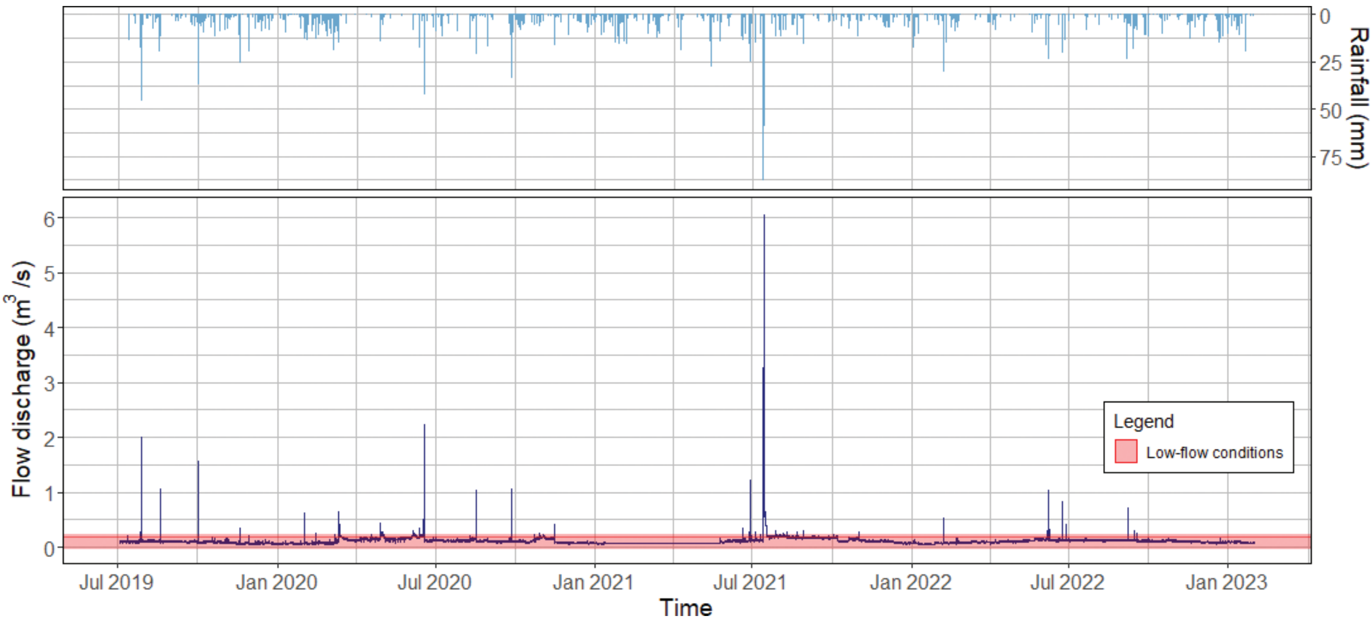

Figure 6. Flow hydrograph and precipitation for the period July 2019–January 2023. Flow varies between 0.03 and 6 m^3/s. A low-flow condition in the Noor brook is marked in red, indicating low flow conditions of 0.19 m^3/s matching 95% probability of occurrence.

Since water level records are constrained to a single monitoring location, a depth-to-width ratio (D/W ratio) analysis of the Noor brook was conducted to provide initial qualitative context regarding morphological heterogeneity and deeply-incised channel sections. Figure 7 illustrates the relationship between the depth and width of the Noor brook in the studied section, from 502 to 1138 m upstream of the Dutch/Belgian border. The larger the depth-to-width ratio (D/W ratio) at a specific location, the deeper the brook is in comparison to its width.

Model setup

Hydraulic characterisation of the brook

In order to calculate the hydraulic characteristics in multiple locations along the brook bed, HEC-RAS was employed to simulate steady flow conditions (Brunner, 2020a). Since hydrodynamic modelling was used for a relatively small brook reach, it was decided to use a high-resolution LiDAR-based Digital Elevation Model from the Dutch 'Actueel Hoogtebestand Nederland' (AHN3, 2025) with a spatial resolution of 0.5 × 0.5 m and altitudinal accuracy of 5 cm. In total, 1074 metres of brook stretch were simulated, including 12 detailed cross sections surveyed in the field along this reach (Woolderink & Harkema, 2023). A representation of the model domain is provided in Figure 8.

Under steady state restrictions, flow is assumed stationary and in equilibrium (Brunner, 2020b). Therefore, flow discharge remained constant throughout the entire length of the brook. Additionally, external fluxes such as groundwater seepage, tributary flow and precipitation were excluded.

Water levels at the upstream part of the model domain were considered sufficient as the upstream boundary condition of the HEC-RAS model. For the downstream boundary condition, energy slope values were approximated by the average slope of the brook in the vicinity of the section (Shields, 1936), following procedures described in the HEC-RAS Reference Manuals (Brunner, 2020a, 2020b). Based on a detailed morphology study on the Noor brook conducted by Woolderink and Harkema (2023),

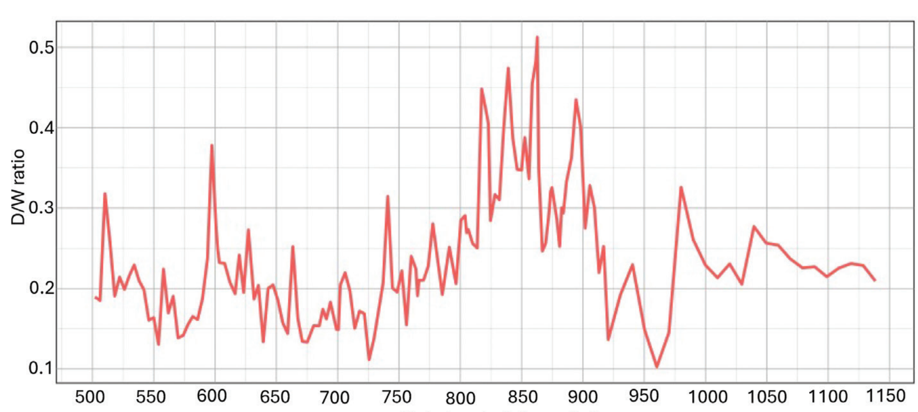

Figure 7. Main brook distance in m from Dutch/Belgian border against the depth-to-width ratio. A larger ratio is attributed to deeper and steeper incision into the substrate.

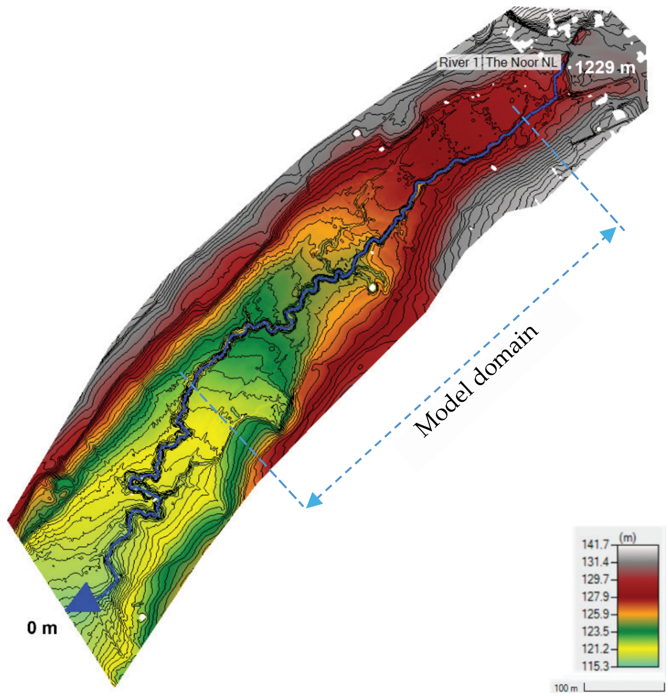

Figure 8. The Noor brook and model domain of the research area in HEC-RAS. HEC-RAS: Hydrologic Engineering Center's River Analysis System.

a brook bed slope of 0.0048 m/m was calculated near the end of the model domain.

Given the relatively steep brook slope and high flow velocities, it was decided to perform model calculations under subcritical, critical and supercritical flow regimes. The HEC-RAS model therefore aimed at revealing the hydraulic characteristics in different locations of the brook using the maximum and median peak flow discharges.

Important for one-dimensional steady state models is the calibration of Manning coefficients considering that hydraulic computations are sensitive to the brook bed roughness. This roughness value is subject to change both spatially and temporally based on water level fluctuations, flow discharges and the conditions of the brook. It can also evolve over time due to the continuous modification of the river cross-sectional areas due to erosion and sedimentation. The calibration of the roughness coefficient aimed at minimising the absolute difference between calculated and observed water levels at the monitoring well in relation to the flow discharge. To avoid a forceful fit of the model with unrealistic Manning coefficients, calibration utilised roughness values consistent with current descriptions of the brook, ranging from 0.03 to 0.05 $s/m^{1/3}$ (Brunner, 2020).

Bedload sediment motion

Reach degradation and stream incision are inherent to bedload sediment motion. Therefore, Shields Stress and Critical Shields Stress were calculated. These two parameters were used to assess whether bedload transport may initiate based on thresholds of motion for specific grain sizes (Simoni & Houlsby, 2006). The bed shear stress at each cross section was calculated to quantify the force exerted on the brook bed by the peak and median flow discharges (see equation 2). The Shields stress is computed to relate the bed shear stress to the critical Shields stress required to initiate sediment particle motion (see equation 3). Thalweg points of the brook were used to calculate a representative bed slope for each cross section. Lastly, while HEC-RAS inherently calculates bedload sediment motion, it was decided to calculate bedload sediment motion outside HEC-RAS to filter the thalweg dataset and avoid computing large slope values over short distances influenced by the presence of pools and riffles.

$$\tau_0 = \rho_w \cdot g \cdot R \cdot S_0 \qquad \text{Equation 2}$$

Where:
τ_0 = Bed shear stress (N/m^2)
ρ_w = water density (kg/m^3)
g = gravity (m/s^2)
R = hydraulic radius (m)
S_0 = bed slope (m/m)

$$\tau^* = \frac{\tau_0}{(\rho_s - \rho_w) \cdot g \cdot D} > \tau_{C*} \qquad \text{Equation 3}$$

Where:
τ_* = Shields stress (–)
τ_{C*} = Critical Shields stress (–)
ρ_s = water density (kg/m^3)
D = sediment particle diameter (m)

A particle diameter of 90% finer sediment grain (D90) was used. This D90 is deemed more relevant than D50 for bedload transport, since the focus is primarily on the susceptibility of the brook to deep incision. Wooldering and Harkema (2023) selected 13 locations along the brook, from which 10 D90 values of the gravel fraction were determined using the sieve method in the field. For consistency of sediment transport calculations, sediment density was set to a general value of 2650 kg/m^3 for both sand and gravel particles (Simoni & Houlsby, 2006). Table 1 shows the D90 values along the brook.

The Shields stress diagram as presented by Parker (2006) was used to set the threshold of motion at each cross section. The kinematic viscosity v was set to 1.002 10^{-6} m^2/s for water with a temperature of 20°C.

Coupling these hydraulic characteristics at each cross section with Shields stress calculations and sediment deficiency allowed to determine the locations of the brook more prone to vertical erosion by means of bedload transport under maximum and median peak flow discharges.

1D Quasi-unsteady state modelling

The essence of quasi-unsteady state modelling lies in simulating a flow series through a sequence of discrete steady flow

Table 1. Sediment sampling and D90 values along the brook.

Distance upstream of Belgian-Dutch border (m)	64	271	298	372	502	701	805	891	1128	1138
D90 (mm)	45	50	50	72	67	50	45	55	90	90

https://doi.org/10.70712/NJG.v105.14028

regime calculations. The main distinction from full unsteady state approach is that quasi-unsteady state approximates the hydrograph by calculating flow over time through a sequence of small, discrete differential time steps, while following steady-state assumptions at each interval. Because of its simplicity, quasi-unsteady state is more stable and less prone to producing numerical artefacts than the full unsteady state approach. Therefore, it was decided to follow the methodology of quasi-unsteady state modelling for the Noor.

The brook schematics, as established for steady state modelling, served as the foundation geometry for simulating sediment transport dynamics. For the hydrodynamic portion, a representative flow series is required as the upstream boundary condition. Due to the lack of reliable continuous inter-annual flow series data, it was decided to replicate a representative observed hydrograph from a single year. As can be seen in Figure 6, the calendar year 2020 experienced peak flow discharges around the long-term median value. To get a time series long enough for the model calculations, this year 2020 was selected and repeated five times. This dataset was considered to be representative for median peak event. The peak discharge of July 2021 was selected as the maximum peak discharge event. The downstream boundary condition was created by calculating a rating curve, based on the hydraulic characterisation of the brook. This was done to capture feedbacks between an evolving bed elevation and water surface levels.

Sediment transport dynamics in HEC-RAS are addressed through the sediment continuity equation, known as the Exner equation (equation 4), which translates sediment deficit into bed erosion and sediment surplus into deposition for a given control volume (Gibson & Hancock, 2019).

$$(1-\lambda_p)\,.\,B\frac{\delta\eta}{\delta t}=-\frac{\delta Q_s}{\delta x} \qquad \text{Equation 4}$$

Where:
λ_p = active porosity of the layer (–)
B = channel width (m)
η = channel elevation (m)
t = time (s)
x = distance (m)
Q_s = transport sediment load (m^3/s)

The Noor brook originates at the St. Brigid spring and, by nature, it does not bring sediment into the system under baseflow conditions. Yet, because the model domain is located downstream of the spring, sediment may already be supplied by remobilisation of brook bed sediments or from the bank material in the upper reaches of the brook. To this date, there are no data available on sediment transport load or flow-sediment concentration at any point in the Noor brook, which may limit the model reliability. For these reasons, the equilibrium load boundary condition was used in order to estimate incoming sediments based on the local transport capacity of the flow and bed gradation at the upstream boundary. This boundary condition assumes zero-gradient concentration normal to the boundary. Therefore, the equilibrium load offers a practical approximation of incoming sediments to address the absence of a lack of data on flow-sediment concentration.

For setting initial conditions on grain size distribution of sediments, specific bed gradations were attributed to each cross section. Campuzano (2017) delineated three bed gradation types in the mid-section of the model area: upstream, midstream and downstream. The more fine-grained sediment type was found in the upstream section and the more coarse-grained sediment type in the downstream section of the model. See Figure 9 for a detailed overview of the grain size distribution.

This grain size distribution was borrowed from Woolderink and Harkema (2023). Along the brook bedding, 13 locations were selected to sample bedding material. The lithology, shape of the cobbles, D50 gravel class and D90 of the gravel were determined at all locations. The authors indicated that it is difficult to obtain reliable D50 estimations of the gravel fraction. Most of the gravel lies in the range of moderately coarse gravel. They also found that the upstream section falls in the fine category (Figure 9A) and the downstream section in the coarse category (Figure 9C).

For this study, the Meyer-Peter Müller (MPM) bedload transport function was chosen over the Einstein-Brown (Okoli et al., 2009) and Wilcock and Crow (2003) approach. MPM is a classical approach for high-slope gravel bed rivers and establishes a direct proportionality between transport and the excess of the Shields parameter above the critical value (Brunner, 2020a, 2020b). HEC-RAS uses the version of MPM introduced by Vanoni (1975), including a drag form correction, for computing transport based on the bed shear stress component acting on the sediment grains.

Two critical components of sediment dynamics are embedded within sediment transport functions and are subject to the modeller's criteria: (1) particle falling velocity and (2) bed sorting method. Fall velocity plays an important role in determining whether sediment particles will deposit in the brook bed or be

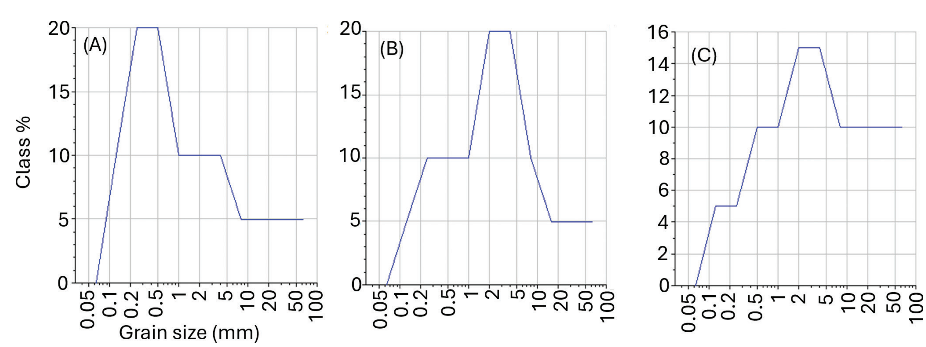

Figure 9. Grain size class percentages for the model area with (A) fine, (B) medium and (C) coarse (adapted from (Vanoni, 1975)).

https://doi.org/10.70712/NJG.v105.14028

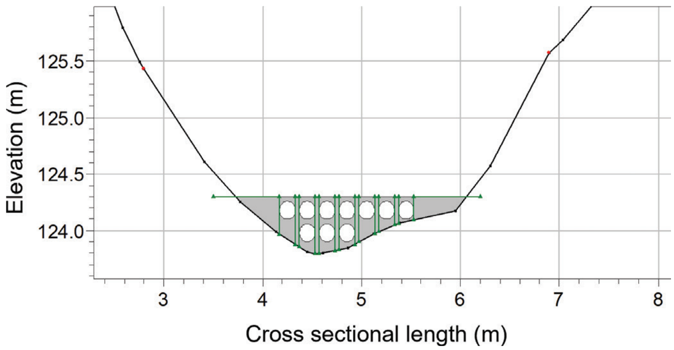

Figure 10. Representation of a gabion dam implemented in HEC-RAS. Circular culverts approximate 30% porosity of the embankment in the cross-sectional area. Flow at the dam is restricted to culvert and overflow only, by defining ineffective flow areas. HEC-RAS: Hydrologic Engineering Center's River Analysis System.

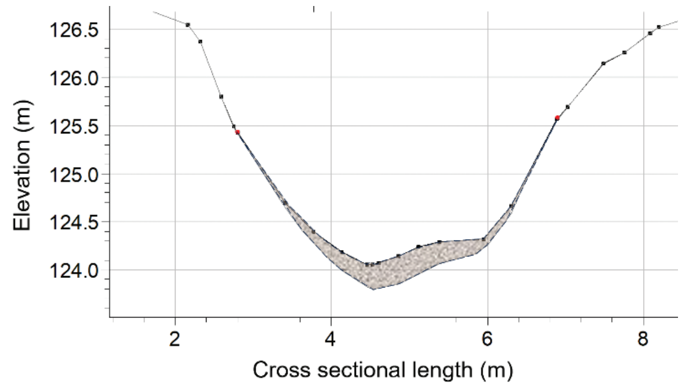

Figure 11. Representation of a cross section of interest for gravel armouring that has been subject to a gradual bed elevation rise that tapers off towards the brook banks.

further transported downstream by flowing water. For this study, it was decided to employ the Van Rijn (1993) falling velocity method due to its development on non-spherical grain particles and shape factor pertinent to natural sand. Regarding the bed sorting method, this component defines the sediment bed active layer subject to sediment transport, continuously tracking the evolving bed gradation over time. Among the two methods available in HEC-RAS, it was decided to employ the Thomas sorting method (1982) due to its flexibility to define multi-layer bed gradations and implement artificial bed armouring.

Implementation of mitigation practices

As a first step, gabion dams in HEC-RAS were represented by inline embankments established at the cross sections. Because HEC-RAS does not explicitly allow the incorporation of porous embankments such as gabion dams, circular culverts were subsequently added into the embankments as a first order approximation of the 30% porosity typical of cobble-based gabion dams (64–256 mm; Berney et al., 2001; see Figure 10). The implementation of culverts followed a simple approach, given the inherent limitations of HEC-RAS regarding the number of discrete culverts and ineffective flow areas that can be designated to a specific cross section in the model domain. This prevents explicitly representing the large number of paths the flow navigates through the porosity of gabion dams. Friction losses along the culvert included entrance and exit losses as well as friction losses calculated using the manning equation for both partial and full flow conditions. Gabion dams were treated as permanently fixed-bed features by designating their locations as passthrough nodes, thereby preventing any bed aggradation or degradation at their locations.

Artificial bed armouring is implemented as the second erosion mitigation practice due to its ability to reduce the transport capacity of the bed sediments. Similar to gabion dams, HEC-RAS does not provide a module to explicitly incorporate river nourishment with material for armouring purposes. In order to account for gravel augmentation in 1D steady state modelling, the brook bed elevation was therefore adjusted to reflect the expected rise of the thalweg (see Figure 11). A mixture of grain sizes was used for the 1D steady state modelling to reduce the porosity of the armouring layer. Particularly, in order to be able to calculate the long-term impact of a brook bed infill with a grain size composition that can withstand peak discharges, a grain size composition was created that combined a low hydraulic conductivity by using fine grained material and a high resistance to erosion by mixing with coarse material.

Results

Long-term hydrogeological conditions of the Noorbeemden

Historical records of deep groundwater levels in the Vaals Formation show a response to a yearly seasonality in recharge and a response to (multiple) wet and dry years. In particular, the groundwater levels close to the deeply incised Noor brook (monitoring well B034) show a clear declining trend of ~1.2 cm year^{-1} from 1993 to 2009 (see Figure 12), in comparison with the relatively constant water head in the Vaals Formation further from the brook (monitoring well B3A). This difference in head trends is attributed to the accelerated lowering of groundwater levels closer to the brook. Since the area does not experience groundwater extractions or soil excavations, the loss in water pressure head is attributed to the continuous brook bed incision and thinning of the resistant clay layer under the brook bed. On the other hand, the short-term linear trend from 2021 to 2025 shows an abrupt increase in deep groundwater levels. This behaviour is primarily related to heavy rainfalls in 2024, accumulating an annual precipitation of over 1200 mm.

On the other hand, shallow water levels in the valley fill further from the brook (piezometer B003) do not show a clear yearly seasonality when compared to deep groundwater levels. Additionally, larger fluctuations are found closer to the brook, which relate to the strong response to the surface flow discharge in the Noor brook. In contrast, smoother temporal behaviour of shallow groundwater levels is found in the valley filling further from the brook, indicating that during summer, the lack of rain surplus is compensated by seepage fluxes. The quick rise in phreatic water level from 2022 onwards at B3 strongly relates to the infill of nearby Noor tributaries.

Hence, a correlation can be drawn between the continuous brook incision, the drop in deep groundwater levels and the response of the shallow groundwater levels. As the brook incision continues, it weakens the hydraulic resistance of the brook bed, resulting in an evident drop in deep groundwater heads near the brook. Additionally, the subsequent larger pressure gradient under the brook alters the direction of the water flow paths redirecting the groundwater increasingly towards the Noor brook. By protecting the remaining clay layer in the brook bed with an infill, an armouring layer and/or

https://doi.org/10.70712/NJG.v105.14028

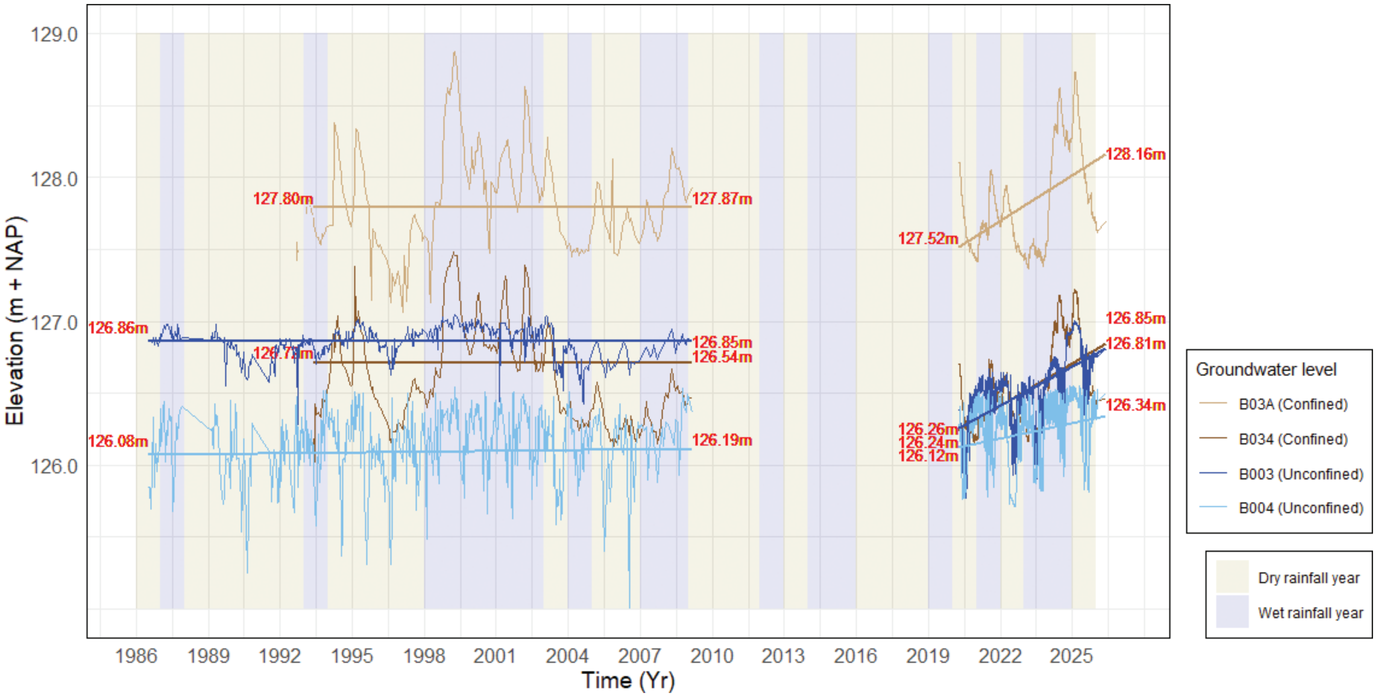

Figure 12. Deep (confined) and shallow (unconfined) groundwater head records and long-term linear trends from 1986 to 2009 and short-term trends from 2021 to 2025. Two monitoring wells with filter screens into the confined Vaals Formations are depicted: (1) B03A, located 50 m away from the bank and (2) B034, located 12.5 m away from the bank. Two additional monitoring wells in the unconfined aquifer are present: B003, adjacent to well B03A, and B003, adjacent to well B034. Start and end values for the linear trend are listed. A calendar year with ≤ 844 mm precipitation is considered dry and > 844 mm, wet year.

gabion dams, a further drop of the deep-water level can be avoided. It is expected that the deep groundwater level will at least stabilise at the current level (no downward trend anymore), but hopefully even a rising trend. This rising trend then can be attributed to (1) the vertical resistance of the poorly sorted fine-grained infill and (2) the higher water level in the brook (see Figure 12). The impact of the vertical resistance of the infill might be limited. A layer of 30 cm fine-grained poorly sorted glacial till-like material would bring a vertical resistance of ~30 days, which is minimal, compared to the estimated 500–1000 days for the valley fill clay. The introduction of such infill with gravel armouring with a total thickness of 30 cm at the thalweg would result in a corresponding water level rise of up to 30 cm. This will have impact on the phreatic water levels close to the brook (possibly also up to 30 cm water level rise) and related to that also a higher water level in the Vaals Formation.

Vulnerability of the Noor brook

Hydraulic channel characteristics for targeted water levels were calculated (see Table 2), presenting the highest flow velocities the upstream sections. Near the monitoring well, velocities range from 0.78 to 2.4 m/s for the median (0.5 m^3/s) and maximum (~ 6 m^3/s) peak flow discharges, respectively. Along the brook, water depth reaches its maximum at the downstream end of the brook, where the brook bed slope is less steep. Similarly, the energy grade line slope exhibits a downstream trend towards the end of the brook. This result aligns with the natural behaviour of flow in open channels, where energy dissipates as it travels downstream.

For the period July 2019–February 2023, the discharge values range from 0.038 to 6 m^3/s (see Figure 6), with velocities up to

Table 2. Hydraulic parameters of the Noor brook at the monitoring well.

Hydraulic characteristic	Max	Median
Water level (m)	0.98	0.34
A (m^2)	2.52	0.64
R (m)	0.49	0.24
V (m/s)	2.4	0.78
Q (m^3/s)	6.06	0.49
n (s/$m^{1/3}$)	0.04	0.04
Sf (m/m)	0.02398	0.0064

2.4 m/s. The maximum discharge was recorded on 14 July 2021 and pertains to the exceptional 2-day rainfall event of 150 mm in the Noor catchment area. With respect to regular peak flow discharges, the time to peak is often a matter of minutes due to the closeness to the flow discharge source. Both the rising and recession limbs of most of the peak flow events are pronounced, representing short, yet intense events. In the extreme, the peak of the flow discharges only lasts up to 30 minutes.

The likelihood of flow discharges in the Noor brook was assessed by comparing two FDCs as given in Figure 13. FDC-a (black line) takes 100% of the flow discharge events into account, while FDC-b (red line) is derived by excluding base flow. In this case, base flow is identified as the 95% of events under low-flow conditions. As a result, FDC-b focuses on peak flow discharges. The use of a logarithmic scale for the probability of exceedance provides a better visualisation, highlighting the prevalence of low-flow discharges and the small likelihood of high-flow discharges to occur. For a maximum peak flow discharge of ~ 6 m^3/s, as recorded during

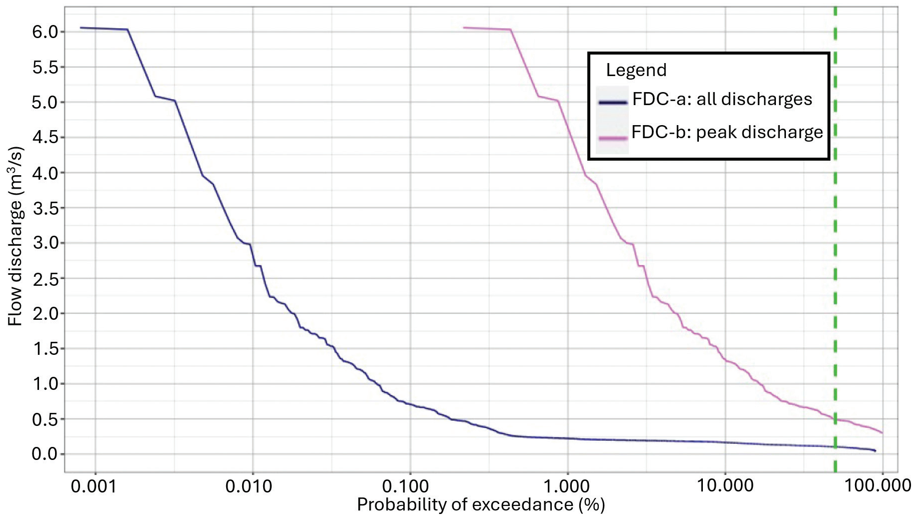

Figure 13. Flow Duration Curves (FDCs) associated with the full range of discharges (FDC-a, black line) occurred in the Noor brook from July 2019 to January 2023 and peak flow discharges representing the 5% highest flows (FDC-b, pink line) occurred during the same time period. Added (green) dashed line intersects both FDCs at 50% probability of exceedance in order to represent the median flow discharge.

mid-July 2021 (see Figure 6), the probability of exceedance is notably low, with a value of 0.001% for FDC-a and 0.2% for FDC-b, respectively. This implies that the maximum peak flow discharge of 6 m^3/s is an isolated, extraordinary event of rare occurrence. A median flow discharge of 0.11 m^3/s can be observed for FDC-a. For peak flow discharges, the median value equals 0.5 m^3/s, with a velocity of 0.8 m/s. In the model analysis section, results for the maximum and median peak discharge are shown for comparison purposes. However, the emphasis relied on the median discharge as its occurrence is considered more representative for assessing the continuous vulnerability of the Noor.

Modelling results

Bedload sediment motion

The particle Reynolds number ranges from 38,300 to 108,400 for gravel particles of 45 mm in diameter and larger. This indicates a critical shield stress ($\tau_* C$) in the range of 0.0295–0.03. Shield stresses (τ_*) for both maximum and median peak flow discharges are compared to the threshold of motion for the specific D_{90}. For peak discharge event of July 2021 of ~ 6 m^3/s, *D90* gravel was over the specific threshold of sediment motion ($\tau_{critical}$). Considering that the morphology and sediment gradation of the analysed sections are representative to the brook as a whole, these results indicate that 90% of the current sediments in the brook are subject to erosion during a discharge event of such magnitude. On the other hand, for a median flow discharge of 0.5 m^3/s, only in the mid-section with the deepest incision *D90* gravel will experience a higher stress than that required for sediment motion (see Figure 14).

Figure 15 shows the calculated minimum grain size required in order to avoid its mobilisation. Under the maximum peak flow discharge (~ 6 m^3/s), grain sizes of at least 160 mm in diameter are required to withstand the shield stress in the most upstream section of the brook. As expected, the need for large cobbles decreases downstream. The median peak flow discharge required grain sizes of up to 70 mm in the middle portion of the brook. A mitigating strategy that aims at protecting the vulnerable clay layer at all times would require an armouring layer with cobbles of at least 160 mm. This would not align with the desire to use local material that does not deviate too much from the grain size distribution in the current brook bed. With a probability of exceedance of 0.2% (excluding base flow) for the July 2021 event, the risk of such an event is also very limited. Therefore an armouring layer of poorly sorted material with the largest stones of up to 70 mm in size which will be able to protect the vulnerable clay layer during median peak events is the preferred mitigation strategy.

Baseline model development

For the calibration of the Manning coefficient, it was considered that the Noor brook is not in a free-flowing state due to the presence of vegetation and extra debris on the banks increasing hydraulic roughness during high flow discharges. Therefore, water level calibration tryouts utilised roughness values that were selected considering a range of 0.03–0.05 for mountain streams with presence of gravels and cobbles in the brook bed and vegetated banks. A manning coefficient of 0.03 $s/m^{1/3}$ was identified to be an adequate value for low-flow conditions (0.2 m^3/s), while larger values at the brook banks appeared to be a better fit for high flows. For this reason, a composite roughness coefficient was defined for the brook cross section as a function of flow discharge. Through an iterative process, the roughness coefficient for the main brook was set to 0.03 considering low-flow conditions, and to 0.045 for both banks considering high-flow conditions.

Figure 16 shows simulated water levels using multiple manning coefficients against the observed water levels from 24 May 2021 to 31 January 2023. Here, the slope of the linear regression for the roughness coefficient composite is the closest to a 1:1 ratio, proving to simulate observed values better than single roughness coefficient values. However, the consistent coefficients of determination (R^2) close to 1 for all simulations, indicate that the observed water levels could be explained by any of the roughness coefficient values. This demonstrates that

https://doi.org/10.70712/NJG.v105.14028

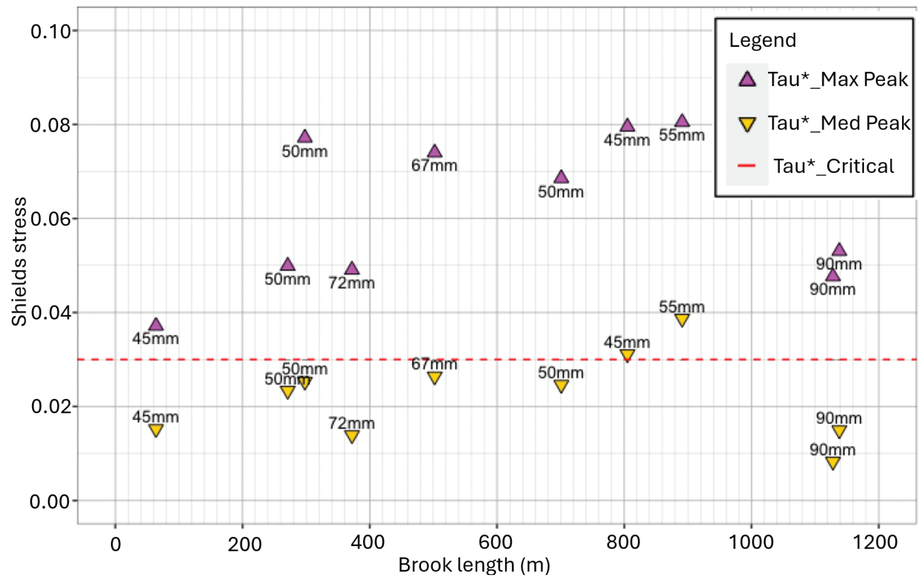

Figure 14. Potential for bedload sediment motion during maximum (Tau*_Max Peak; > 6 m³/s; July 2021 rain event) and median (Tau*_Med Peak; 0.5 m³/s) peak flow discharges along the Noor brook. Maximum peak flow discharge is shown because the July 2021 event occurred within the available time period. This extraordinary event is excluded from the dataset to get to a realistic median peak as input for the HEC-RAS modelling exercise. The brook length is given from the Dutch/Belgian border (0 m) to the St. Brigid spring (1200 m upstream). At each location, values in mm represent the D90 sediment diameter, while τ* indicates the calculated shield stress. For the *D90* sediment particles, the threshold of motion was determined to be 0.03. HEC-RAS: Hydrologic Engineering Center's River Analysis System.

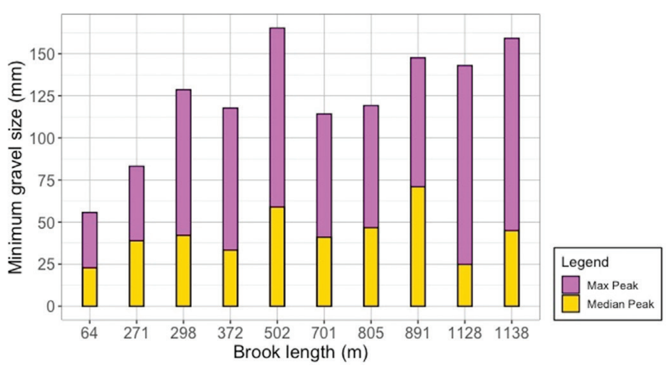

Figure 15. Minimum gravel diameters required along the brook, from downstream (left end) to upstream (right end). Gravel diameters for maximum peak flow discharge of ~ 6 m3/s are shown with purple bars. The overlapping gold bars represent gravel diameters for the median peak flow discharge of 0.5 m3/s.

the simulated water levels were only weakly sensitive to the tested roughness range (n = 0.03–0.05). Nevertheless, it is important to consider the relatively small-scale brook and its associated small water level variations. In such cases, a higher level of precision may be desirable.

Implementation of mitigation practices

The impact of gabion dams on the backwater profiles was studied by introducing a gabion dam at 602, 700, 765, 805, 822, 851, 862, 873 and 882 m upstream from the Dutch/Belgian border (see Figure 17). These locations were chosen in relation to the brook bed gradient. In steeper segments, the gabion dams were placed closer to each other. At these locations, the upstream area of influence is relatively short in comparison to areas in which the brook gradient represents a gentler slope. In section 850–890 m, one of the steepest sections of the brook, an overall slope of 0.03 m/m was found. A width of 50 cm is attributed to all gabion dams. In addition, three options with different gabion dam heights were explored: 30, 50 and 70 cm.

In the upstream section, a gabion dam of 30 cm high in a relatively gentle slope section did not show significant impacts on water levels. On the other hand, gabion dams of 50 and 70 cm height showed a surface water level increase of 5 and 12 cm. In the steepest segment, the impact of the gabion dams is relatively high. An increase of up to 37 (30 cm dam height), 48 (50 cm dam) and 58 cm (70 cm dam) is found. The introduction of gabion dams in this segment implicates an increase in water level related to water retention, causing a desired reduction in flow velocity and a lower Froude number. The taller the gabion dam, the lower the flow velocity becomes, and it is likely that a subcritical flow regime will be observed.

The introduction of gravel armouring followed a standard armouring thickness of 30 cm at the thalweg, resulting in a corresponding water level rise of 30 cm. Although reductions in flow velocity are evident, with water flowing through the armouring bed, they are not sufficient to allow for a transition to subcritical flow. The armouring bed gentles the bed slope creating a reservoir-like area that reduces the flow velocity from 0.7–1.4 m/s to 0.4–0.6 m/s. This significant reduction directly translates to a higher water profile. In areas with gentle slopes, a rise in bed elevation due to a 30 cm gravel armouring results in a similar water level increase (~30 cm) over the added gravel armour.

1D Quasi-unsteady state modelling

Considering the erosive nature of the brook, the calibration of the quasi-unsteady simulation was focused on the expected bed volume change of the brook related to the erosion rate of the brook bed. According to Mesman (2019), the riverbed elevation of the Noor brook is subject to a decreasing rate of 8.5 mm/y, which goes in hand with field observations in the period 2012–2014 (8–10 mm/y).

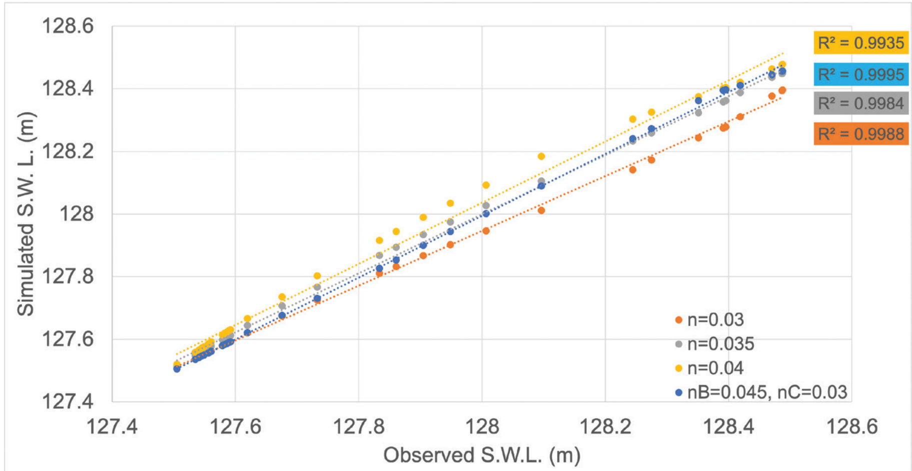

Figure 16. Comparison of linear regressions for simulated versus observed surface water levels for the period 24 May 2021 – 31 January 2023, with varying roughness coefficients. Best fit is provided by the roughness coefficient composite of 0.03 at brook bed and 0.045 at brook banks.

The result of the long-term quasi-unsteady state simulation yields a total sediment balance of 64 m^3/y, which under median flow conditions equals an erosion rate of 12 mm/y. A difference between observed erosion rates of 8–10 mm/y and calculated rates of 12 mm/y is deemed to be acceptable given the notoriously uncertain sediment transport functions. Additionally, it is common for transport computations to vary by at least one order of magnitude (Dust & Wohl, 2012). Thus, despite the erosion and deposition in multiple areas, the Noor brook is overall an erosive brook (Figure 17). This behaviour goes in hand with the nature of the St. Brigid spring as the spring itself does not bring sediments into the brook. Particles in motion come from the banks and/or the brook bed. The dominant grain class in the sediment transport dynamics is found to be fine sand, followed by very fine sand (VFS). Sediment particles smaller than VFS, such as clay, are not shown to be representative for erosion and deposition patterns. Moreover, in the upstream part of the brook, transport of larger grains such as very fine gravel and medium-sized gravel also occurs. This can be related to the steeper brook bed gradients.

The implementation of gabion dams does not alter the erosive nature of the Noor in its entirety. However, a significant reduction in erosion behaviour compared to the situation without gabion dams can be observed. Gabion dams with a 30 cm height demonstrate a significant (60%) erosion reduction. There are no significant differences between the 50 and 70 cm gabion dams, but they show an erosion reduction of >80%. The dominant grain sizes under sediment transport fall within the category of fine sands (FS in Figure 18), followed by VFS.

The implementation of gravel armouring yields contrasting results in comparison to any gabion dam scenario. Yet, a similar pattern of sediment deposition and reduced erosion can be noted upstream of each gravel armour implementation. This is likely associated with the simplified introduction of gravel armouring in HEC-RAS as seen by the abrupt change in elevation when rising the brook bed. Overall, gravel armouring

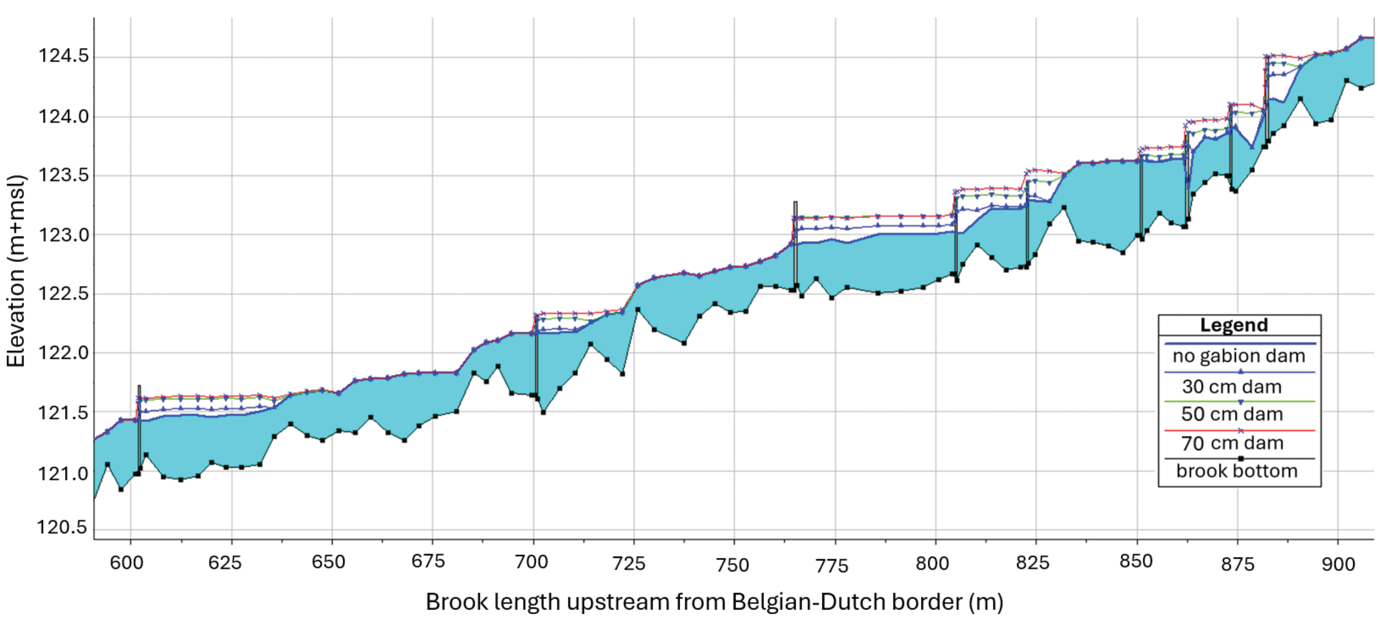

Figure 17. Water levels related to the simulation of gabion dams with a height of 30, 50 and 70 cm respectively. Simulated backwater effect is also shown.

https://doi.org/10.70712/NJG.v105.14028

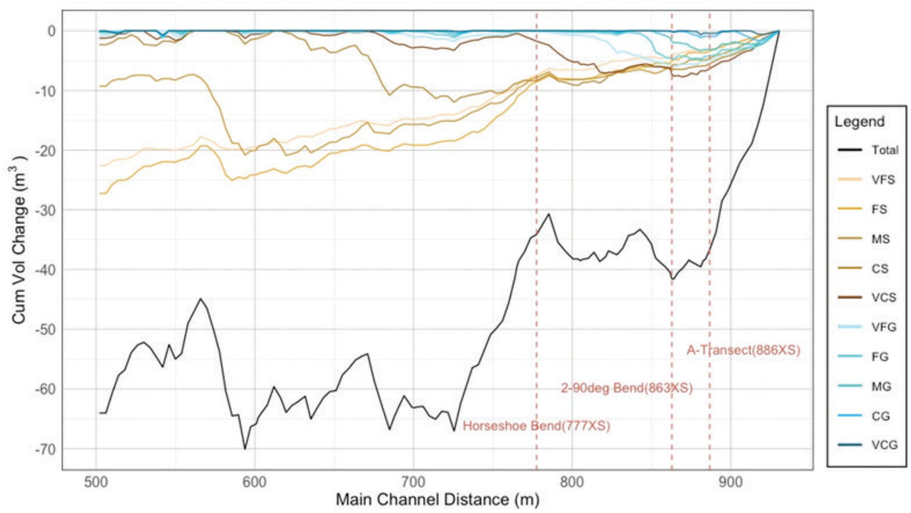

Figure 18. The longitudinal cumulative volume change from upstream (right end) to downstream (left end) of the brook is illustrated for the total sediment transport as well as by grain class. The Noor yields a total sediment balance –64.2 m3, indicative of an overall erosive system.

simulations caused an apparent larger erosion along the brook. While the brook bed was protected from erosive fluvial forces, the larger sediment volume transport is associated with the fine material eroded from within the armouring layer itself. The dominant grain sizes under sediment transport fall within the category of fine sands, for grains with diameters of 0.0625–0.125 mm. Additionally, VFSs to medium sands represent 93% of the total eroded volume.

No implementation of erosion mitigation leads to a further incision of the brook bed, which will have a detrimental impact on the shallow and deep groundwater levels near the brook. The impact of peak discharge might be reduced by the creation of retention reservoirs for sewage spills. Gravel armouring in the deeply incised sections of the brook will protect the clay layer from further erosion. Cobbles of up to 160 mm would create a stable armouring bed, even for the maximum measured peak discharge of 6 m^3/s. However, given that the probability of exceedance of the maximum peak discharge is very low, this maximum peak flow event is left out. Therefore, medium peak discharges of 0.5 m^3/s were taken as starting point for the armouring layer assessment. The HEC_RAS modelling exercise showed that a cobble size of 70 mm is sufficient to keep the armouring layer stable under these conditions.

Results indicate a positive impact when considering gabion dams as a mitigation practice. To start with, an almost null change in bed elevation, signifying complete erosion mitigation, can be observed when the gravelly armour layer is combined with a series of gabion dams at the downstream side of the armouring layer. Gabion dams with a height of 30 cm demonstrate a significant impact in erosion mitigation. Gabion dams with a height of 50 and 70 cm show a 50% stronger impact on erosion reduction, but the difference between 50 and 70 cm gabion dams is minimal. Also, the calculated impact of the dams on the surface water level when a 50 cm or 70 cm dam was applied was minimal. Given these results, it was concluded that the optimal cost/impact ratio is found with dams of 50 cm. A 70 cm gabion dam would have a similar impact on flow velocity and erosion/sedimentation as a 50 cm gabion dam, yet it would have a larger environmental impact (a bigger disturbance of the current profile).

Discussion

Discharge was calculated from a historical record of surface water levels at a specific point in the upstream section of the Noor brook. These discharges were used for the bedload motion calculations and 1D steady and quasi-unsteady state analysis. Therefore, water level measurements and subsequent calculated discharges may be subject to a temporal bias due to the evolving morphology. It is likely that small retention reservoirs might develop under low-flow or no-flow conditions due to the formation of pools and riffles. This behaviour could potentially lead to water level readings that suggest the occurrence of discharge, thereby affecting the flow hydrograph and subsequent sediment transport dynamics. Lastly, the calibration of the roughness coefficient during the development of the baseline model could not be validated at multiple locations or other variables due to constraints in data availability. Therefore, the implementation of a composite roughness coefficient could not be conclusively demonstrated in comparison to other roughness values tested. For this reason, results should be interpreted as a first-order estimation.

Sediment transport dynamics for the entire length of the brook were quantified using a flow discharge series constrained by water level observations at a single monitoring location. Spatially, this neglects the occurrence of tributary flow contributions, which might lead to an increased discharge and increased brook bed erosion. It can also lead to brook bank collapses, resulting in significant sediment pulses into the brook. However, the section that has been tested with HEC-RAS does not have any tributaries of any importance. Therefore, it is expected that this assumption will not have a significant impact on the results. Temporally, replicating the flow time series from a single year was done to emphasise median peak flow conditions provided the lack of continuous inter-annual flow time series data. This provides a first-order representation of morphological response under median long-term peak discharges. However, it does not account for inter-annual variability, threshold behaviour, or hysteresis effects, all of which are associated with non-linear morphological changes. This way, results should be deemed illustrative rather than predictive.

With regards to sediment transport boundary conditions used in this study, the equilibrium load upstream boundary condition assumes that sufficient sediment is available to satisfy local transport capacity. This condition considers that the flowing water is not sediment-starved at this location, which may reduce the sediment deficit in the model domain and overall erosion. Even though the equilibrium load boundary condition was required to approximate the incoming sediment load due to absence of field data, future work should include a sensitivity analysis utilising other boundary conditions, such as the clear water or zero sediment supply, especially when study domains are close to or start at the spring source. While field data are necessary, such analyses can strengthen erosion and deposition patterns results.

Continuous detailed monitoring of the research area is recommended. Regular surveys on changes of brook cross sections over time, flow discharge measurements at multiple locations along the brook, and detailed sampling of bed gradations remain essential aspects to consider. Such additional data would provide valuable input for the calibration of both hydrodynamic and sediment transport modelling frameworks. For instance, continuous long-term flow series records are crucial for capturing the temporal variability in the morphodynamic feedback loop when simulating multi-year sediment transport dynamics.

The implementation of gravel armouring and gabion dams within this study followed general understanding of their construction and composition. Additionally, the general functionality of such mitigation practices on protecting the brook bed is perceived. Nevertheless, both erosion mitigation techniques require further development within modelling frameworks. While gabion dams do not explicitly resolve the distributed internal flow paths through the gabion matrix, simulations captured the dominant hydraulic controls (i.e. upstream ponding) and general erosion and deposition patterns. This way, culverts represent a simplified approach of the porous media with fundamental limitations. Flow contraction, expansion and wall friction losses are considered, yet the current approach neglects the tortuosity and drag effects through rockfill porous media. As a result, frictional losses, water levels, and associated sediment deposition are likely underestimated, particularly under high flow conditions. Future modelling efforts should incorporate more physically representative formulations to describe flow through porous media, such as the Forchheimer equation, or exploring distributed porosity formulations available in two-dimensional models.

As for gravel armouring, the modelling framework should follow a more detailed procedure in order to fully capture the response of bed armouring to erosion and deposition processes. Although sediment deposition was observed upstream the armoured section, this may be due to the abrupt change in elevation when rising the brook bed. Further modelling efforts should establish an appropriate armouring gradation and incorporate a more realistic, gradual transition from brook bed to the armoured layer.

Conclusion

In the case of an extraordinary peak discharge such as that of July 2021 (150 mm), there is no gravel diameter sampled in the Noor that can withstand the erosive force of a peak discharge exceeding 6 m^3/s. This fact does not imply that deep incision is imminent. While the intensity of this maximum peak flow is relevant, it has an almost null probability of occurrence, making this an isolated event. Therefore, this discharge should not be considered a target for sustainable erosion mitigation practices. Instead, focusing on the median peak flow discharge facilitates the identification of susceptible areas to bedload transport. Bedload sediment motion calculations under median peak discharge coincide with observed deeply incised areas, and results on smaller gravel size requirements can make erosion mitigation practices more realistic. It also broadens the options to utilise local material for gabion dams and/or armouring layers.

One-dimensional quasi-unsteady HEC-RAS modelling provides a simplified representation of gravel armouring and gabion dams with fundamental limitations in resolving flow-sediment-structure interactions. Further modelling improvements are required for capturing morphodynamic feedbacks more explicitly. Nevertheless, results indicate that gabion dams with a height of 50 cm, when strategically placed, yield the most beneficial impact in mitigating deep incision. The subsequent sediment deposition increases the brook bed elevation, which can help maintain the base-rich upward seepage essential for the local flora of the Natura 2000 area, Noorbeemden.

It is crucial to consider the Noor as a dynamic system. Hydraulics, sediment composition, morphology and aquatic biota are subject to vary both in space and time. Regardless of the mitigation practice employed, the changes of variability in sediment composition over time can create niches for macroinvertebrates to thrive in multiple areas in the brook.

Author contributions

Conceptualisation, R.D. and B.R.C.; methodology, R.D. and B.R.C.; Validation: B.R.C.; formal analysis, R.D.; original draft preparation, R.D.; writing-review and editing: B.R.C.; visualisation: R.D. and B.R.C.; supervision: R.D.

Acknowledgments

The authors acknowledge H. Wooldeink and T. Harkema for their detailed analysis of the brook bed by doing intensive fieldwork and a lab analysis on grain distribution of the brook bed sediments.

Conflicts of interest

The authors declare no conflicts of interest.

References

AHN3, 2025. Algemeen Hoogtebestand Nederland, Developed 2014–2019. Accessed October 2023, www.ahn.nl.

Arcgisonline, 2025. arcgisonline/hoogteviewer. Accessed 28 May 2025, www.arcgisonline.nl/hoogteviewer.

Berney, O., Charman, J., Kostove, L., Minetti, L., Stoutesdijk, J. & Tricoli, D., 2001. Small dams and weirs in earth and gabion materials. Food and Agriculture Organization of the United Nations (FAO-UN), Rome, Italy.

Brunner, G.W., 2020a. HEC-RAS River Analysis System: hydraulic reference manual version 6.0. US Army Corps of Engineers-Hydrologic Engineering Center, pp. 133–134, Davis, CA, USA.

Brunner, G.W., 2020b. HEC-RAS River Analysis System: HEC-RAS user's manual version 6.0. US Army Corps of Engineers-Hydrologic Engineering Center, p. 77, Davis, CA, USA.

Campuzano, I.G., 2017. Are woody debris jams suitable to prevent the Noor brook bed erosion? Groundwater and bank erosion impacts. MSc thesis, Hydrology and Environmental Hydroulics, Wageningen University.

Chardon, V., Schmitt, L., Arnaud, F., Piegay, H. & Clutier, A., 2021. Efficiency and sustainability of gravel augmentation to restore large regulated rivers: insights from three experiments on the Rhine river (France/Germany). Geomorphology **380**: 107639. DOI: 10.1016/j.geomorph.2021.107639

Dinoloket, 2025. Dinoloket.nl/REGIS. Accessed 29 May 2025, www.dinoloket.nl/REGIS.

Dijksma, R. & Van Lanen, H.A.J., 2001. De afvoer van de Noor (Zuid-Limburg): periode 1992–2000 (No. 98). Landbouwuniversiteit Wageningen, Wageningen, the Netherlands.

Dust, D. & Wohl, E., 2012. Conceptual model for complex river responses using an expanded Lane's relation. Geomorphology **139:** 109–121. DOI: 10.1016/j.geomorph.2011.10.008

Gibson, A. & Hancock, G., 2019. Suspended sediment load estimation in an ungauged river in southeastern Australia. River Research and Applications **36**(4): 512–521. DOI: 10.1002/rra.3558

Grabowski, R.C., Gurnell, A.M., Burgess-Gamble, L., England, J., Holland, D., Klaar, M. & Wharton, G.J., 2019. The current state of the use of large wood in river restoration and management. Water and Environment Journal **33**(3): 366–377. DOI: 10.1111/wej.12465

Hariri, H., Hosseini, S.A. & Khosrojerdi, A., 2022. Evaluating gabion performance in sediment yield reduction of basin under current and future conditions (case study Dehbar Basin). Arabian Journal of Geosciences **15**: 402. DOI: 10.1007/s12517-022-09694-z

Ikhsan, C., Permana, A.S. & Negara, A.S., 2022. Armor layer uniformity and thickness in stationary conditions with steady uniform flow. Civil Engineering Journal **8**(6): 1086–1099. DOI: 10.28991/CEJ-2022-08-06-01

Kessels, K.G.W., 2012. Ecohydrology of the Noorbrook catchment; effect of the incised Noorbrook on the spatial distribution of groundwater within the Noorbeemden and its consequences for the nature reserve. MSc thesis, Hydrology and Environmental Hydraulics, Wageningen University.

Knighton, D., 2014. Fluvial forms and processes: a new perspective. Routledge, p. 306, Dept. of Geography, University of Sheffield, Sheffield, UK.

KNMI, 2025. Royal Dutch Meteorological Institute. Accessed 6 May 2025. knmi.nl

Manners, R.B., Doyle, M.W. & Small, M.J., 2007. Structure and hydraulics of natural woody debris jams. Water Resources Research **43:** WO6432. DOI: 10.1029/2006WR004910

Merz, J.E. & Ochikubo Chan, L.K., 2005. Effects of gravel augmentation on macroinvertebrate assemblages in a regulated California River. River Resource Applications **21**: 61–74. DOI: 10.1002/rra.819

Mesman, B., 2019. The effects of small woody debris jams on the morphology of the Noor brook. MSc thesis, Hydrology and Environmental Hydraulics, Wageningen University.

Moreno Gómez, M., Ghysels, G., Mustafa, S.M.Y., Six, S., Vandenbohede, A., Diez, T., Cirkel, D.G. & Huysmans, M., 2025. Spatial variability of hydraulic conductivity of the Cretaceous aquifer in Belgium. Journal of Hydrology: Regional Studies **60**: 102462. DOI: 10.1016/j.ejrh.2025.102462

Natura2000, 2025. Accessed 28 May 2025. Natura2000.nl/gebieden/limburg/noorbeemden-hoogbos

Okoli, C.S., Ojo, S.I.A. & Oguntuase, A.M., 2009. Modelling of sediment transport capacities of Ogbese and Owena rivers in S.W. Nigeria. Advanced Materials Research **62–64**: 786–796. DOI: 10.4028/www.scientific.net/amr.62-64.786

Parker, G., 2006. 1D sediment transport morphodynamics with applications to rivers and turbidity currents, St. Anthony Falls Laboratory, University of Minnesota, Minneapolis, MN, USA.

Pasternack, G.B., Wang, C.L. & Merz, J.E., 2004. Application of a 2D hydrodynamic model to design of reach-scale spawning gravel replenishment on the Mokelumne River, California. River Research and Applications **20**(2): 205–225. DOI: 10.1002/rra.748

Pitlick, J., Mueller, E.R., Segura, C., Cress, R. & Torizzo, M., 2008. Relation between flow, surface-layer armoring and sediment transport in gravel-bed rivers. Earth Surface Processes and Landforms: The Journal of the British Geomorphological Research Group **33**(8): 1192–1209. DOI: 10.1002/esp.1607

Roni, P., Beechie, T., Pess, G. & Hanson K., 2015. Wood placement in river restoration: fact, fiction, and future direction. Canadian Journal of Fisheries and Aquatic Sciences **72**(3): 466–478. DOI: 10.1139/cjfas-2014-0344

Shields, A., 1936. Application of similarity principles and turbulence research to bed-load movement, Mitteilungen der Preussischer Versuchsanstalt fur Wasserbau und Schiffbau, Berlin, Germany. Translated by Soil Conservation Service, Cooperative Laboratory, California, Institute of Technology, Pasadena, CA, USA (translated by W.P. Ott and J.C. van Uchelen).

Simoni, A. & Houlsby, G.T., 2006. The direct shear strength and dilatancy of sand-gravel mixtures. Geotechnical and Geological Engineering **24**: 523–549. DOI: 10.1007/s10706-004-5832-6

Staentzel, C., Beisel, J.N., Gallet, S., Hardion, L., Barillier, A. & Combroux, I., 2018. A multiscale assessment protocol to quantify effects of restoration works on alluvial vegetation communities. Ecological Indicators **90**: 643–652. DOI: 10.1016/j.ecolind.2018.03.050

Thomas, W.A., 1982. Mathematical modeling of sediment movement. In: R.D. Hey, J.C. Bathurst & C.R. Thorne (eds.). Gravel-bed rivers, fluvial processes, engineering and management. John Wiley, pp. 487–511, Oxford, UK.

Tiernego, M., 2010. Flow routes in a deeply incised brook system; a case study in the Noor Valley, South Limburg. MSc thesis, Hydrology and Environmental hydraulics, Wageningen University.

Vaezi, A., Rostami, K. & Sadeghi, S.H.R., 2021. Investigation on the effectiveness of gabion check dams in amount and grain size of sedimentation in the Rezin watershed, west of Iran. Journal of Water and Soil Conservation **27**(5): 201–216. DOI: 10.22069/JWSC.2020.17747.3328

Van Lanen, H.A.J. & Dijksma, R., 1999. Water flow and nitrate transport to a groundwater-fed stream in the Belgian-Dutch chalk region. Hydrological Processes **13**(3): 295–307. DOI: 10.1002/(SICI)1099-1085(19990228)13:3%3C295::AID-HYP739%3E3.0.CO;2-O

Van Lanen, H.A.J., Van de Weerd, B., Dijksma, R., Ten Dam, H.J. & Bier, G., 1995. Hydrogeologie van het stroomgebied van de Noor en de effecten van grondwater onttrekkingen aan de westrand van het Plateau van Margraten (Hydrogeology of the Noor catchment and the impact of groundwater abstractions at the western edge of the Margraten Plateau (in Dutch)). Research report 57. Wageningen University, Wageningen, the Netherlands.

Van Rijn, L.C., 1993. Principles of sediment transport in rivers, estuaries and coastal seas, Aqua Publications, Blokzijl, the Netherlands (www.aquapublications.nl).

Vanoni, V.A., 1975. River dynamics. Advances in Applied Mechanics **15**: 1–87. DOI: 10.1016/S0065-2156(08)70055-3

Wallerstein, N., Thorne, C.R. & Doyle, M.W., 1997. Spatial distribution and impact of large woody debris in northern Mississippi. In: Proceedings of the Conference on Management of Landscapes Disturbed by Channel Incision, University of Mississippi, pp. 145–150, May 19-23-1997, Oxford, Mississippi, USA. (Editors: S.Y. Wang, E.J. Langendoen and F.D. Shields Jr.).

Wang, Q., Pan, Y., Yang, K. & Nie, R., 2020. Structural properties of the static armor during formation and reestablishment on gravel-bed rivers. Water **12**: 1845. DOI: 10.3390/w12071845

Wilcock, P.R. & Crowe, J.C., 2003. Surface-based transport model for mixed-size sediment. Journal of Hydraulic Engineering **129**(2): 120–128. DOI: 10.1061/(ASCE)0733-9429(2003)129:2(120)

Woolderink, H.A.G. & Harkema, T.T.L., 2023. Morfodynamiek van de Noor (Morphodynamics of the Noor (in Dutch). Wageningen Environmental Research Report, 52 pp, Wageningen, the Netherlands.

Zhou, Z., Coco, G., Townend, I., Olabarrieta, M., Van Der Wegen, M., Gong, Z. & Zhang, C., 2017. Is 'morphodynamic equilibrium' an oxymoron? Earth-Science Reviews **165**: 257–267. DOI: 10.1016/j.earscirev.2016.12.002